BB

CEA/SACLAY
DSM

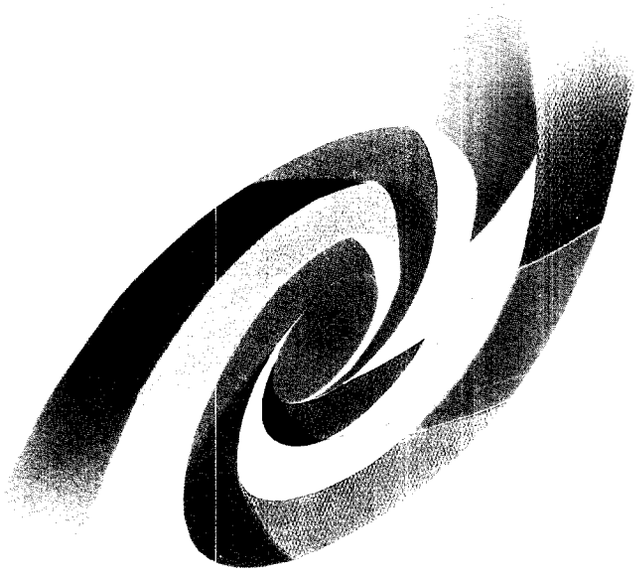

SW9743

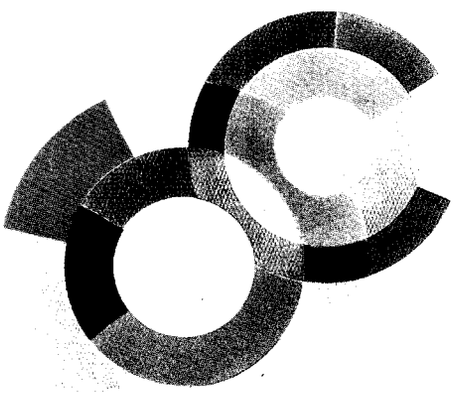

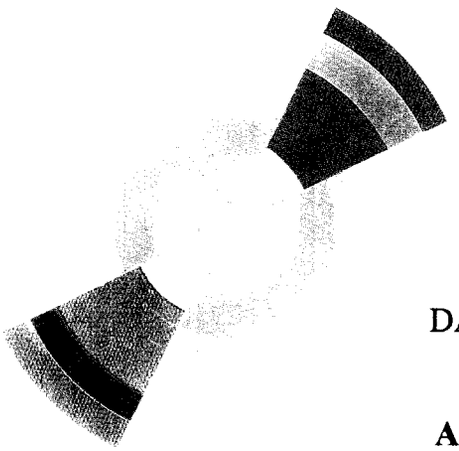

DAPNIA/SPhN-97-23 04/1997

A velocity spectra study for light particles (LP) emitted in the reaction $^{40}Ar(44\ MeV/n) + ^{27}Al$ by means of the multidetector Argos

G. Lanzano, E. De Filippo, M. Geraci, A. Pagano, S. Aiello,
A. Cunsolo, R. Fonte, A. Foti, M.L. Sperduto,
C. Volant, J.L. Charvet, R. Dayras, R. Legrain,
J. Richert, P. Wagner

DAPNIA

Département d'**A**strophys que, de Physique des **P**articules, de Physique **N**ucléaire et de l'**I**nstrumentation **A**ssociée
CEA/Saclay F-91191 Gif-sur-Yvette Cédex

Couverture Sylvie Cabrit et Marc Sauvage

XXXVth International Winter Meeting on
Nuclear Physics,
BORMIO, Italy, 3-8 February 1997

A velocity spectra study for light particles (LP) emitted in the reaction ^{40}Ar(44 MeV/n)+^{27}Al by means of the multidetector Argos

G. Lanzanò, E. De Filippo, M. Geraci, A. Pagano
S. Aiello, A. Cunsolo, R. Fonte, A. Foti, M.L. Sperduto
Istituto Naz. Fisica Nucleare and Dipartimento di Fisica
Corso Italia 57, 95129 Catania, Italy
C. Volant, J.L. Charvet, R. Dayras, R. Legrain
CEA, DSM/DAPNIA/SPHN, CE-SACLAY, F-91191 Gif-sur-Yvette Cedex, France
J. Richert, P. Wagner
CRN Strasbourg, BP 20 CR, 67037 Strasbourg Cedex, France

April 1, 1997

Abstract

We present a study of the particles emitted in the reaction ^{40}Ar+^{27}Al at 44 MeV/n. In particular, the LP velocity spectra are studied as a function of the detection angle and the forward projectile-like fragment (PLF) charge. By means of a three source analysis we extract temperature slope parameters as a function of the PLF charge and information on the intermediate source in fair agreement with previous published values.

It is also observed that a great amount of the forward detected light charged particles are correlated, and due to the break-up or decay of light excited ions.

Preliminary calculations based on a multisequential decay of an excited ^{40}Ar projectile reproduce quite well the experimental results.

1 Introduction

As known, the study of light particles and light fragments emitted in heavy ion nuclear reactions can give some insight on the involved reaction mechanisms. This is certainly true at low energies, where simple spectra are found, characteristic of the emitting source. By increasing the bombarding energy the experimental particle energy spectra become more complex, suggesting either that a consistent part of the particles are dynamically emitted before thermo-dynamical equilibrium is reached or/and that more than one emitting source is present. The main information relative to their emission or to the properties of the emitting sources, can be extracted from the shape of energy spectra, angular distributions, multiplicity and their relative abundances [1, 2, 3, 4].

In particular, to deepen the reaction mechanism involved in the projectile fragmentation at intermediate energies [5, 6], we have undertaken a series of exclusive experiments with the multidetector ARGOS at different beam energies and using a variety of targets, ranging from Carbon to Thorium. In these experiments the LP velocity spectra were studied in a large angular range in coincidence with PLF detected in the ARGOS forward wall. In addition we studied also the correlations in the forward wall between on the one hand light charged particles (LCP) and LCP, and on the other hand light heavy ion and light heavy ion. In the following, after a description of the ARGOS multidetector and the experimental lay-out, we will concetrate our attention on the LP-PLF coincidence results, by presenting a three source analysis performed on the experimental velocity spectra, mainly for the reaction $^{40}Ar + ^{27}Al$ at 44 MeV/n. Preliminary results concerning the LCP-LCP correlations at forward angles are also presented. Finally, the results are compared with the predictions of a multisequential decay mechanism. For more experimental details on the results presented in this talk, see [7]

2 The multidetector Argos and the E230 experimental layout

Argos is a multidetector, made by 112 separate, hexagonal BaF_2 crystals modifiable into phoswichs, by means of a fast plastic scintillator sheet, of suitable thickness, according to the charge and dynamical range of the ion to be detected [8, 9, 10]. Each crystal has a surface of 25 cm^2 and a thickness variable up to 10 cm, stopping protons of energy up to 200 MeV. Due to its modularity, the array can be arranged to fit different geometries. When the single detector is modified in phoswich, in addition to the light charged particles also heavy ions are detected and identified with a threshold in energy depending on the plastic thickness. Neutron detection is also allowed, with an efficiency depending mainly on the crystal thickness and on the electronic threshold. Typically, neutron efficiency values of about 8% are observed for 5 cm thick crystals and 1 MeV-ee threshold. Timing characteristics of the phoswich detector are well enhanced, reaching values less than about 250 psec resolution, so that precise time-of-flight measurements are possible if suitable flight-paths and good time-resolution starts are available.

The ARGOS multidetector was placed in the Nautilus big scattering chamber at GANIL, with the following geometry. A forward wall of 60 phoswichs was placed between 0.7° and 7° in shape of honeycomb at a distance of 235 cm from the target (solid angle: 0.03 sr); they detected PLF identified in charge and LCP isotopically separated. After linearization of the total light component, mass separation was also achieved for light ions. The angular separation between the centers of two adjacent detectors was $\approx 1.5°$.

A backward wall of 18 phoswichs was placed between 160° and 175° at a distance of 50 cm from the target (solid angle:0.2 sr), for the detection of LCP and neutrons.

A battery of about 30 phoswichs was placed in plane at a distance from the target variable from 2m to 0.5m following the expected counting rate, between 10° and 150°, detecting all the reaction products, the only limiting factor being the different thresholds.

In this experiment we used plastic scintillator thickness of 700 and 30 μm for the

forward wall and the remaining detectors respectively.

Shape discrimination of the Photomultiplier signals and time-of-flight techniques [11] have been exploited for a full identification of all the charged reaction products. An example of the heavy ion charge and LCP isotopic separation achieved is shown in the bidimensional plot of Fig. 1, where the fast component is reported as a function of the time-of-flight. For all detected particles the calibration was made by means of time-of-flight measurements, gamma-rays giving a reference time for the detectors in plane and in the backward wall, the same the elastic scattering for the detectors placed in the forward wall.

In this experiment, the event was recorded every time the in-plane detectors or the backward wall triggered, a minimum multiplicity of 2 being requested.

3 Analysis of the light particles velocity spectra

Fig. 2 shows a typical bidimensional plot of the invariant cross-section, for α-particles in coincidence with Z=16 PLF detected in the forward wall. Two sources are clearly visible, whose velocities are very close respectively to the initial velocities of the projectile (8.9 cm/ns) and the target. However some particles with velocity intermediate between these two are also present in the plot, suggesting the occurrence of dynamically emitted particles from the overlap zone of the two interacting nuclei, that can be thought as a third source of particles. In effects for PLF of charge $\geq$ 9, all the particle energy spectra can be consistently interpreted in the frame of three equilibrated sources . However for LP in coincidence with PLF of charge $\leq$ 8 the evidence of two sources, like in Fig. 2, is less and less clear. On the contrary, we observe an increasing coincidence rate between light heavy ions (see Fig. 3), with a correlation charge peaked near Z=6 (see Fig. 4a), suggesting a more complex decay mechanism for the excited projectile or PLF nucleus, like fission or cracking [12], and accounting for the anomalous light heavy ion rise already observed in inclusive PLF mass and charge distributions [13]. We have then restricted our analysis to events for wich LP were in coincidence with PLF of charge $\geq$9.

By supposing LP emission by three independent moving equilibrated sources, and more precisely a surface emission for the two sources with velocity close to the ones of the projectile (PLF source) and target (TLF source)respectively, and a volume emission for the source with a velocity intermediate between those ones (intermediate source), we have fitted at the same time all the velocity spectra from 1.5° to 175° to the sum of three maxwellians including Coulomb repulsion, two of wich of surface and one of volume [14, 15]. We have applied this fit procedure for each particle species, for each PLF charge and for each target. To show the quality of the fit, some results are presented in Fig. 5a,b,c. Forward and backward emission by an equilibrated excited projectile or PLF is evident at the most forward angles and is fairly well reproduced by the calculation. On the contrary, the emission at the most backward angles is almost totally due to an equilibrated excited target or TLF. Finally the intermediate source dominates at angles close to 40°.

From this fit procedure we have extracted source velocities, temperatures and intensities. Fig. 6 shows the velocity for PLF and TLF sources, averaged on LP species, as a function of the PLF charge. As expected [13], for decreasing values of the PLF

charge the PLF velocity is decreasing, while the velocity of the TLF is increasing. Fig. 7 shows the three source temperatures as a function of the PLF charge and the particle species. Starting from the projectile charge, the temperature of both PLF and TLF sources increases as the PLF charge decreases until a plateau is reached at around 5-7 MeV for Z=9. Furthermore almost the same temperature is found for these two sources and a slight dependence is observed from the particle type. For the intermediate source, if we except the anomalous behaviour of α particles, we find an almost constant temperature of about 14-17 MeV as a function of the PLF charge, as already found in previous inclusive experiments [2]. Fig. 8 shows the LP relative abundance in the three sources for events in which a PLF of charge Z=14 is detected in the forward wall. In general α particles are as much abundant as protons. The important neutron emission for the PLF source is probably connected with the particular nature of the projectile, a neutron rich nucleus. As expected, the intermediate source composition is intermediate between the PLF and TLF sources ones.

4 Preliminary results on the particle-particle correlations at forward angles

As known, the study of two particle correlations at small relative momenta can give some insight on the spatial and temporal extension of the emitting source; further the relative populations of excited states furnishes information on the temperature of that source. This method has been succesfully used to study intermediate velocity highly excited systems produced in intermediate energy heavy ion induced reactions [16, 17]. The extension of the method to the study of highly excited projectiles or PLF is not straightforward, and requires the use of a suitable multidetector, because of the particle high rate and focusing in the forward direction. As described above, due to its fine angular granularity, Argos is a suitable detector for such a kind of studies.

The correlations obtained are very similar to the ones reported in [16] for different couples of LCP. An example for α-α correlations is reported in the bidimensional plot of Fig. 9, showing the α-particle velocity as a function of their relative momentum expressed in MeV/c. The ground state and the broad first excited state of ^{8}Be are clearly visible, and enhanced for α-particle velocities close to the one of the projectile. Fig. 10 gives the relative momenta distribution for a ^{8}Be in its ground state and a third alpha-particle, showing evidence for the existence of excited ^{12}C nuclei (in this case the observed peaks correspond to the first α-particle emitting level at 7.65 MeV and a group of levels at around 10-12 MeV excitation energy) having the beam velocity. The same, Fig. 11 shows the relative momentum distribution for a ^{8}Be in its ground state and a proton, leading to the intense instable ground state of ^{9}B.

From a preliminary analysis, more than 10% of the events involving the detection of at least one α-particle in the forward wall, are due to the break-up of a ^{8}Be.

For ion-ion coincidences and for a fixed charge of one of the two ions, the maximum of correlation is observed for velocities close to the beam velocity, and shifts towards higher relative momenta values as the charge of the coincident ion increases, as shown in Fig. 12 for Z=5 ions.

5 Preliminary multisequential calculations and conclusions

As shown in section 2, we have evidence for two sources, centered at a velocity close to the one of the projectile and target respectively. Although particles with a velocity intermediate between the ones of the two above-said sources are clearly present in Fig. 2, however their origin is not clear, as they could be dinamically emitted from the overlap zone between the two colliding nuclei or by a highly excited and equilibrated nuclear system (fire-ball) formed in the same region. By neglecting this intermediate velocity emission, we can idealize the reaction scenario by supposing that after the reaction a projectile and a target, highly excited and equilibrated, are formed, with an excitation energy distribution depending on the impact parameter. Following the approach of [18, 19], they can after decay by particle emission or fission, with a transition probability given in [15]. We have performed some calculations concerning the projectile decay, by supposing for simplicity a flat temperature distribution from 0 MeV to a maximum temperature value T_{max}, whose value was varied until a satisfactory agreement with the experimental data was obtained. We took into account the detector geometry, the velocity of the primary projectile was assumed the beam one with a gaussian angular distribution centered at 0°. As an example we report in Fig. 4b the ion-ion charge correlation in the forward wall, that reproduces fairly well the maximum near Z=6, see Fig. 4a. Finally Fig. 13 shows the relative abundance of all the reaction products emitted by the decaying projectile as compared to the experimental results. Though the accord with the experimental data is in general good, however the production of Z=3 and Z=4 ions is underestimated.

In conclusion, by means of the multidetector ARGOS we have studied the fate of a 44 MeV/n ^{40}Ar after collision with different targets, mainly ^{27}Al.

For PLF with charge close to the one of the projectile 8<Z<20, two sources are clearly visible. The LP velocity spectra can be successfully reproduced in the whole angular range by the sum of three maxwellians. The slope temperatures so extracted are dependent from the LP species and also from the coincident PLF charge. Almost equal temperatures are observed for PLF and TLF sources. However our data cannot be interpreted in an unambiguous way concerning the intermediate source. Apart α-particles for wich a slight dependence from temperature is observed, for the other LP the temperature is almost constant at around 14-17 MeV.

As the PLF charge decreases, the two sources are not any more distinct and the probability that a PLF has to be accompanied by another (light)-PLF, increases. This fact, probably due to the projectile-fission or cracking for less and less peripheral collisions, accounts for observed inclusive light-mass PLF distribution.

The anomalous abundance of α-particles issued from the reaction could be related to the α-clusterization of light projectiles like Argon. Furthermore, many of them are correlated, following the break-up of light heavy ions.

Finally, preliminary calculations based on a multisequential decay starting from an excited ^{40}Ar projectile, are in a fair agreement with the experimental results.

Acknowledgements

We wish to thank the Ganil machine staff for having provided us with a beam of excellent characteristics. We are also grateful to N. Giudice, N. Guardone, V. Sparti, S. Urso and J.L. Vignet for their assistance during the experiment, and to C. Marchetta for targets preparation.

References

[1] T. C. Awes et al., *Phys. Rev.* **C25** (1982) 2361

[2] B. V. Jacak et al., *Phys. Rev.* **C35** (1987) 1751.

[3] D. Guerreau: "Light particle emission as probe of reaction mechanism and nuclear excitation", Talk presented at the Int. School of Physics, Varenna (Italy) 1989 and Ganil-draft P89-17.

[4] J. Galin: "Hot nuclei studied with high efficiency neutron detectors", Talk presented at the XXI Summer School on Nucl. Phys., Mikolajki(Poland), 1990 and Ganil-draft P90 17.

[5] R. Dayras et al.,*Phys. Rev. Lett.* **62** (1989) 1017.

[6] J.C. Steckmeyer et al. Nucl. Phys. **A500**, 372, (1989).

[7] M. Geraci, Doctoral Thesis (unpublished), Università di Catania, 1997.

[8] G. Lanzanò et al., "Grandi apparati di rivelazione e prospettive della Sez. INFN di Catania", Acireale, pag. 10, 1993

[9] G. Lanzanò et al., *Nucl. Instr. and Meth.* **A323** (1992) 694

[10] E. De Filippo et al., Nuovo Cimento **107A** 775 (1994).

[11] G. Lanzanò et al., *Nucl. Instr. and Meth.* **A312** (1992) 515

[12] J. P. Bondorf, Journal de Physique **C4** 263 (1986).

[13] R. Dayras et al. Nucl. Phys. **A460**, 299 (1986).

[14] A. S. Goldhaber, Phys. Rev. **C17** 2243 (1978).

[15] V. F. Weisskopf, Phys. Rev. **52** 295 (1937).

[16] J. Pochodzalla et al., *Phis. Rev.* **C35**, 1695, (1987)

[17] O. Schapiro and D.H.E. Gross, Nucl. Phys. **A573**, 143, (1994).

[18] C. Barbagallo et al., Z. Phys. **A324**, 97, (1986).

[19] J. Richert et al. Nucl. Phys. **A517**, 399, (1990).

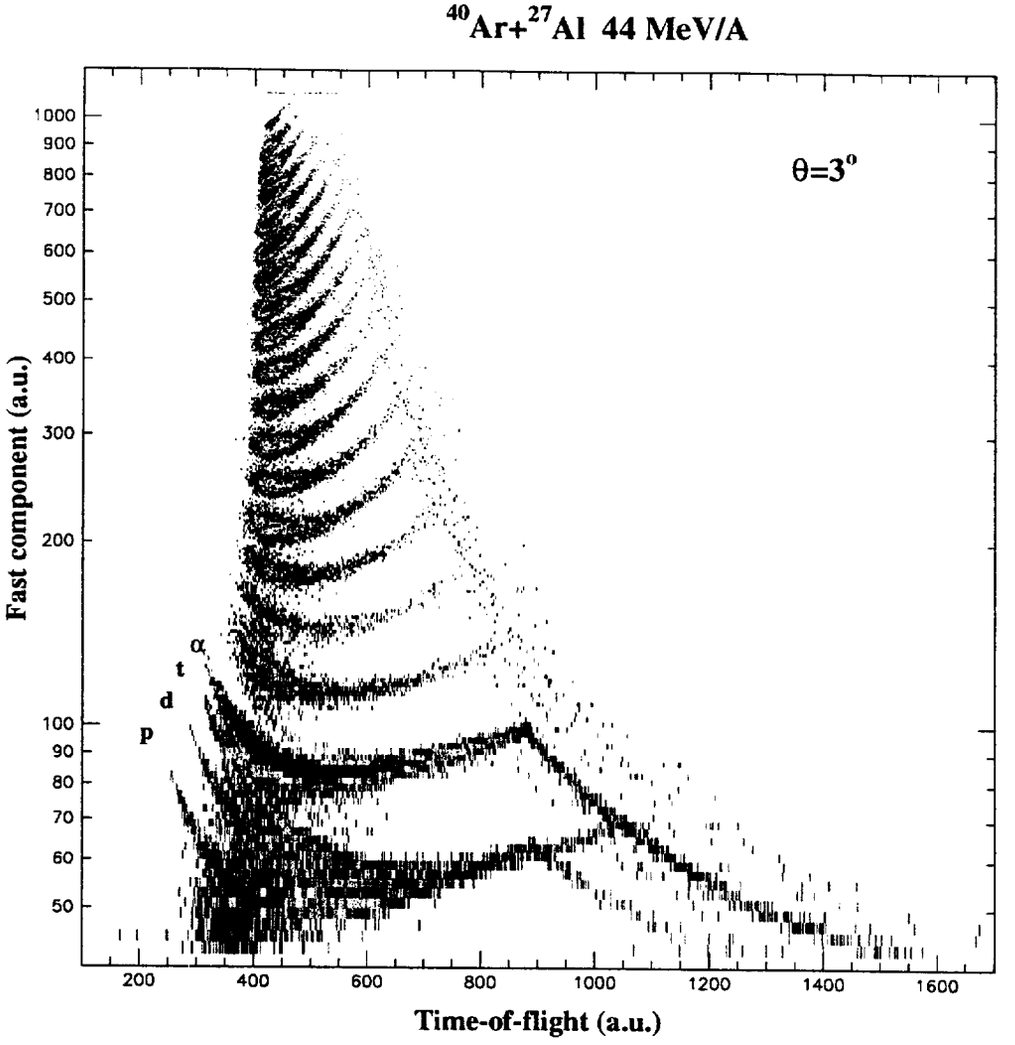

Figure 1: Fast component as a function of time-of-flight for a forward wall BaF_2.

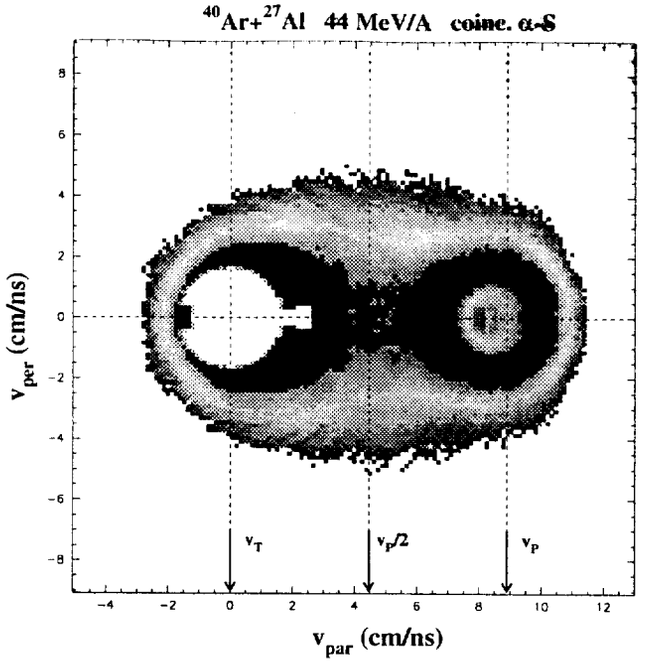

Figure 2: Lorentz invariant cross-section for α particles in coincidence with Z=16 PLF detected in the forward wall. The projectile velocity v_p is 8.9 cm/ns.

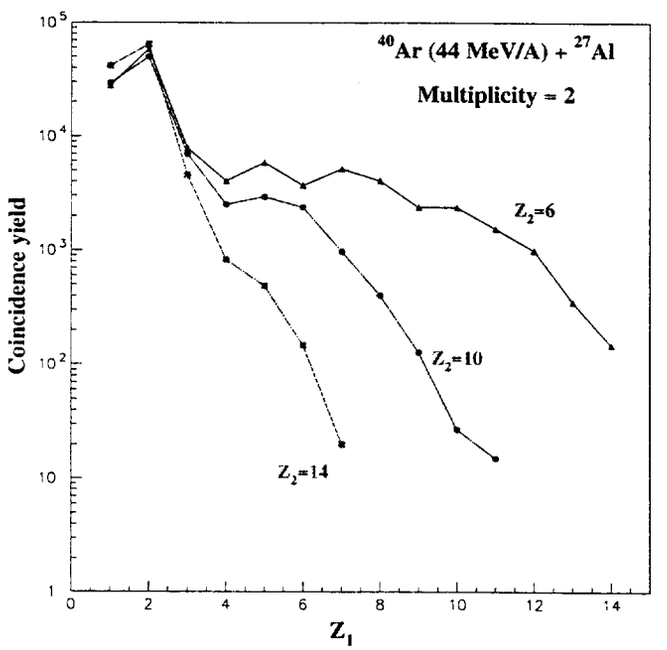

Figure 3: For the selected multiplicity M=2 the PLF production rate of charge Z_2=14,10 and 6 is reported as a function of the coincident PLF charge Z_1.

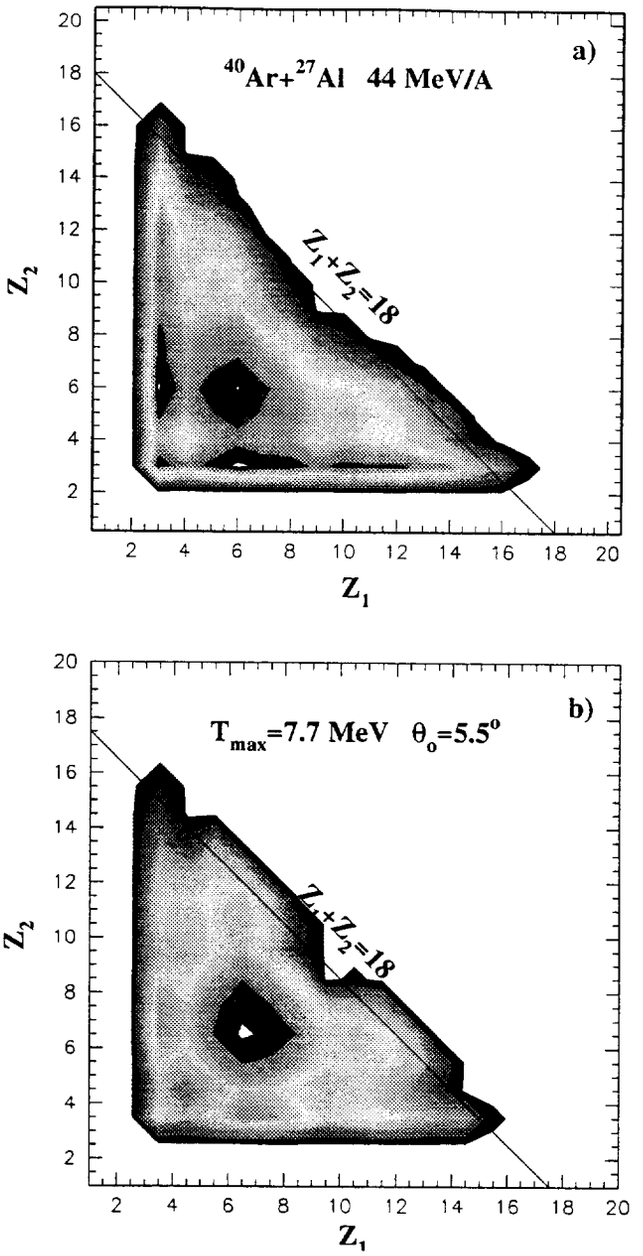

Figure 4: a) Experimental charge-charge PLF correlation in the forward wall for Z1,Z2≥3 and b) Charge-charge PLF correlation as result of a multi-sequential calculation (see text) filtered by the forward wall geometry.

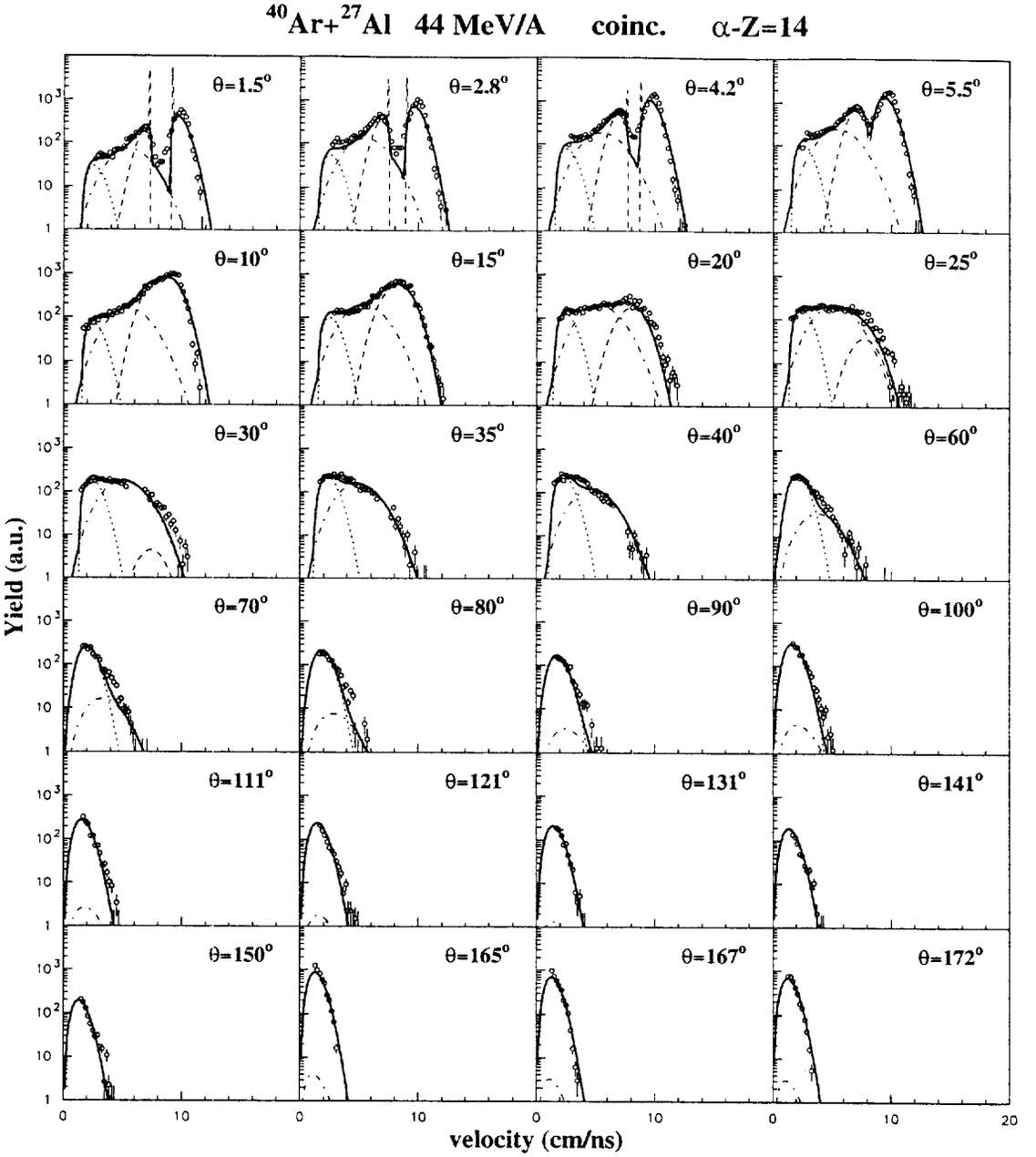

Figure 5: a) α-particle velocity spectra (not normalized) detected from $\theta = 1.5^o$ to $\theta = 172^o$ in coincidence with a Z=14 PLF. The lines are the result of a three equilibrated sources fit procedure; TLF source: dotted line, PLF source: dashed line, Intermediate source: dot-dashed line; Total: thick line. The beam velocity is 8.9 cm/ns.

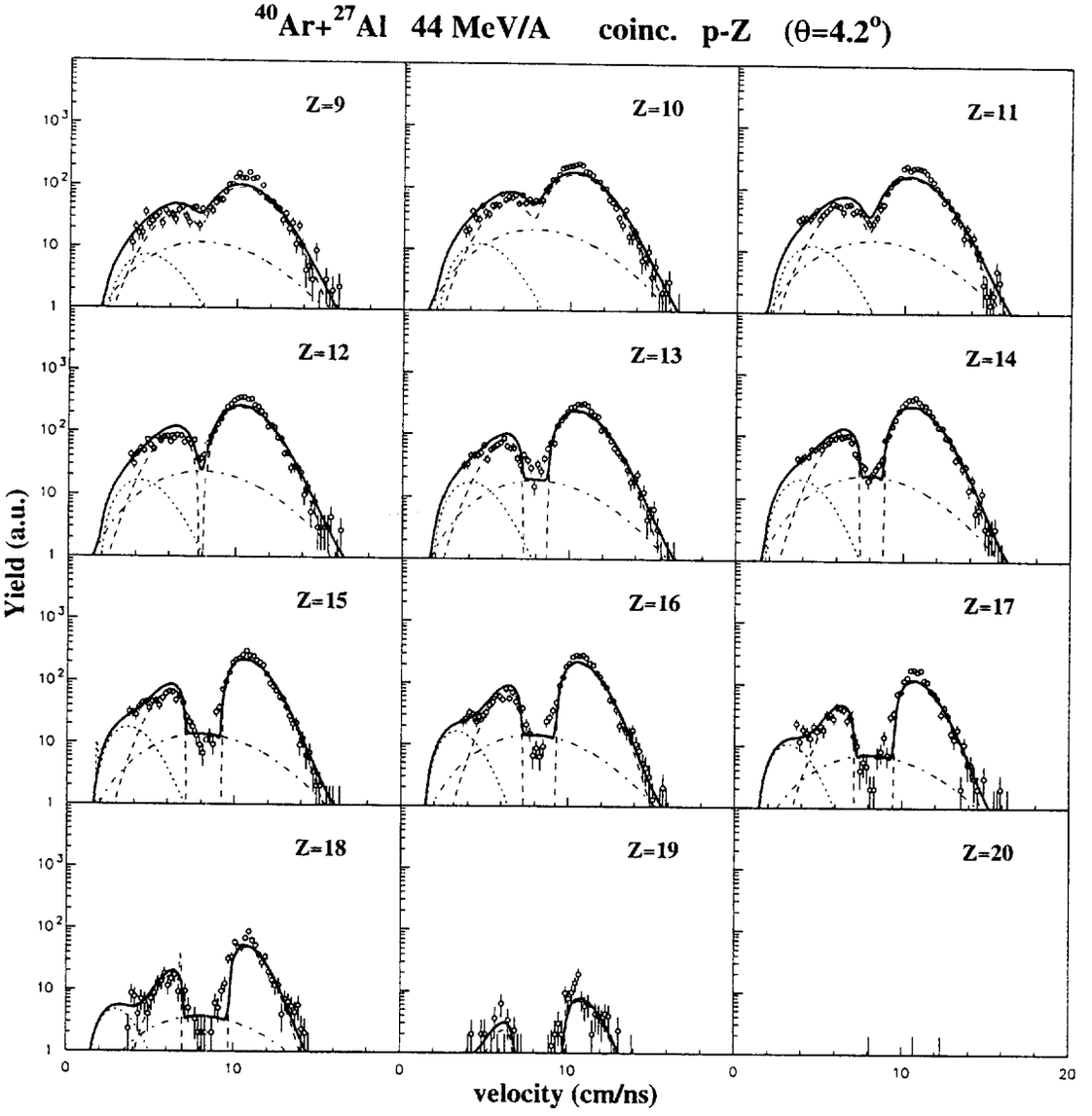

Figure 5: b) Proton velocity spectra (not normalized) detected at $\theta = 4.2°$ in coincidence with a PLF of charge from 9 to 19. The lines are the result of a three equilibrated sources fit procedure; TLF source: dotted line, PLF source: dashed line, Intermediate source: dot-dashed line; Total: thick line.

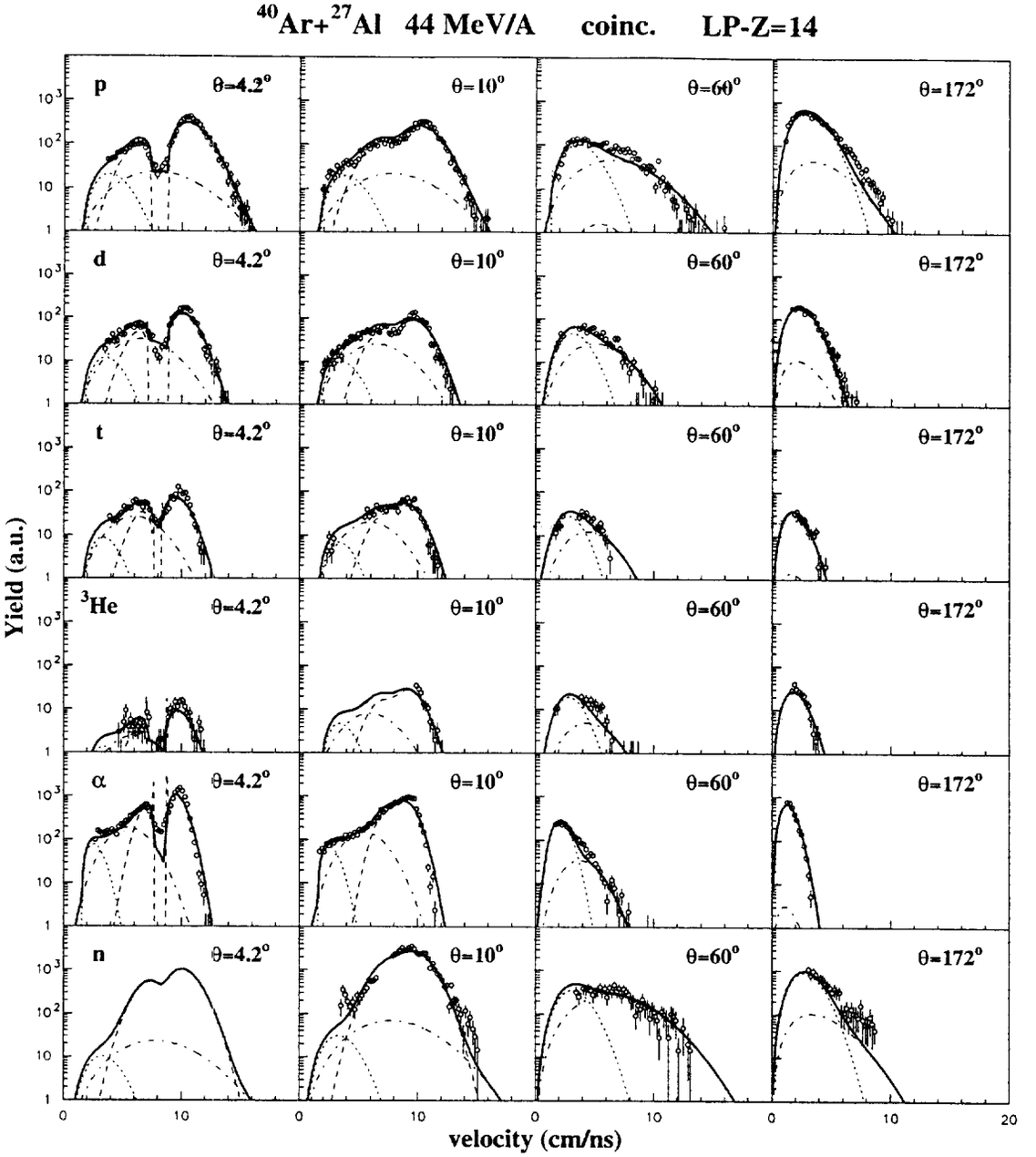

Figure 5: c) Proton, deuteron, triton, ^{3}He, α and neutron velocity spectra (not normalized) detected at $\theta = 4.2°$,10°, 60° and 172° in coincidence with a PLF of charge Z=14. The lines are the result of a three equilibrated sources fit procedure; TLF source: dotted line, PLF source: dashed line, Intermediate source: dot-dashed line; Total: thick line.

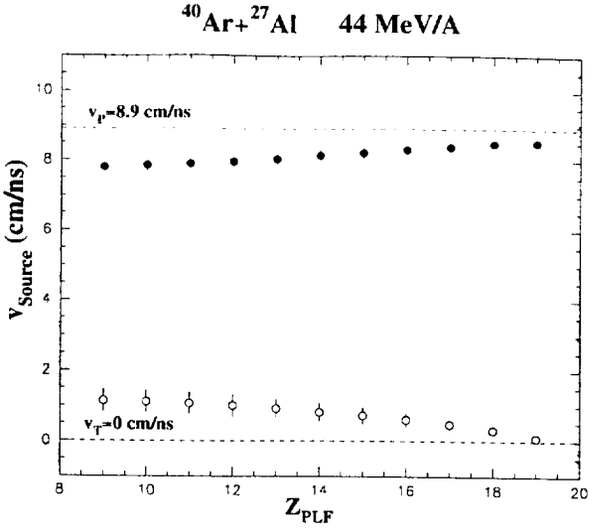

Figure 6: Mean velocity for the PLF and TLF sources as a function of the PLF charge. Velocities are averaged upon the LP species (the error bar indicates the standard deviation). For the fit procedure see text.

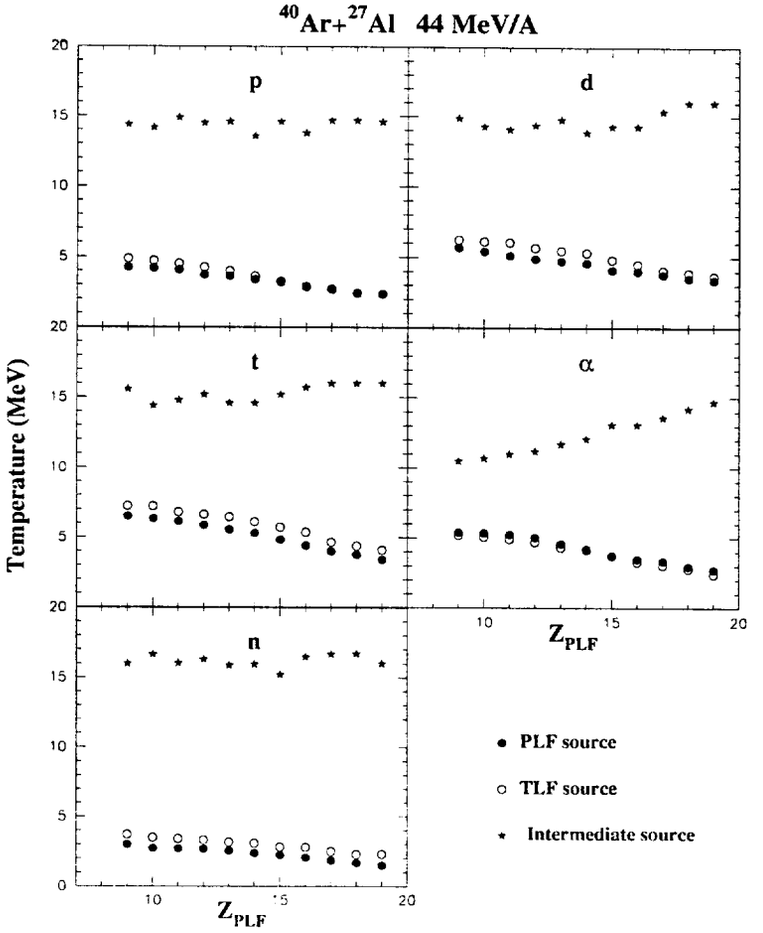

Figure 7: Slope temperatures (obtained from the fit procedure described in the text) are reported as a function of PLF charge for the PLF, TLF and intermediate sources respectively and for all LP.

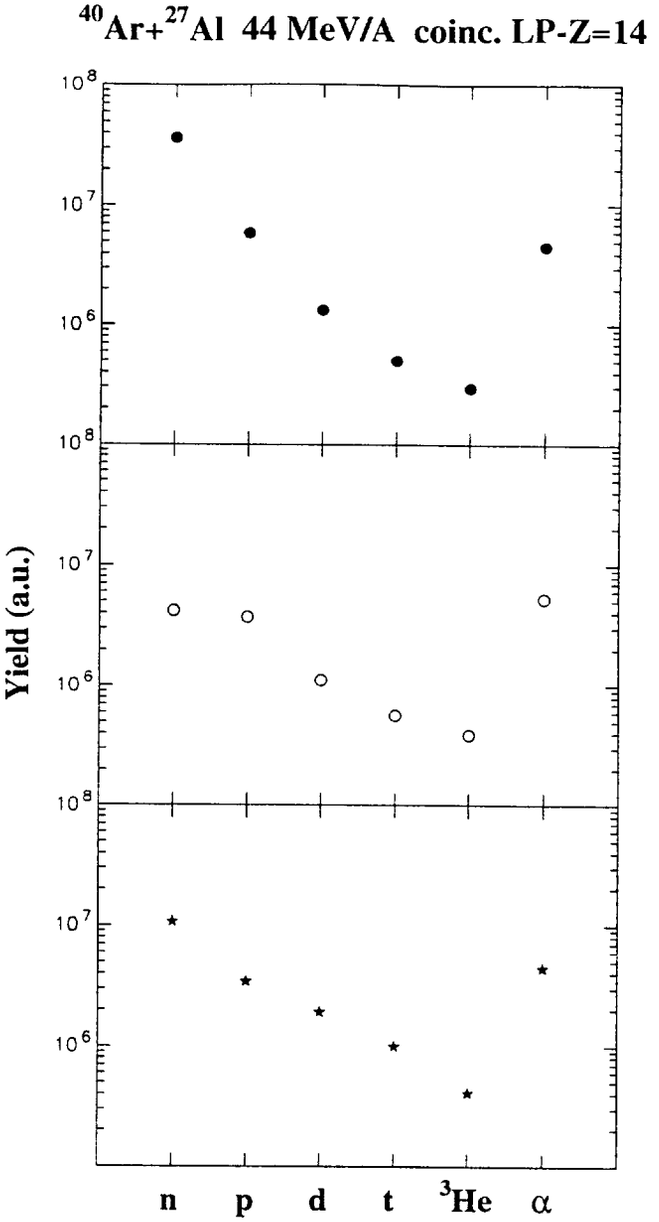

Figure 8: Light particle composition for PLF (full points), TLF (circles) and intermediate source (stars) respectively. Data are results of fit procedures for LP-Z=14 PLF coincidences.

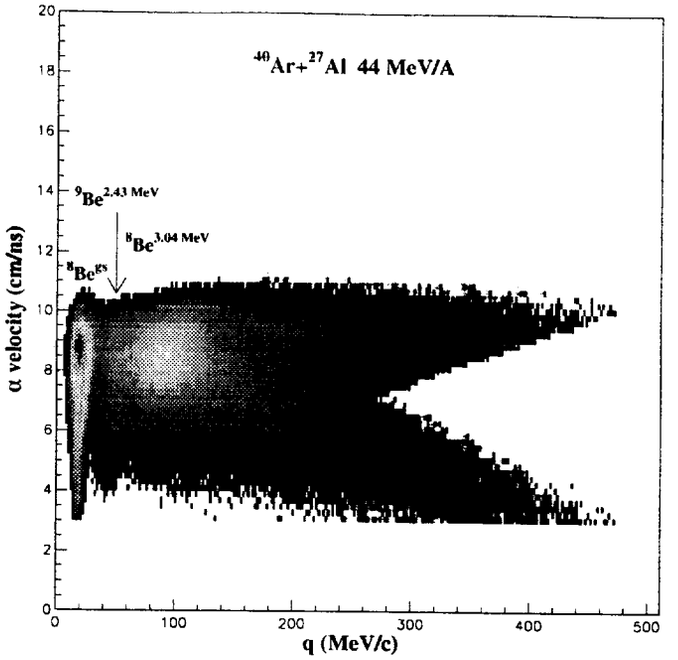

Figure 9: For $\alpha - \alpha$ correlations their velocity is reported as a function of their relative momentum q; besides the ground state and the broad first excited level in ^{8}Be, a structure is also visible at q≈50 MeV/c, associated to the decay of the 2.43 MeV state in ^{9}Be.

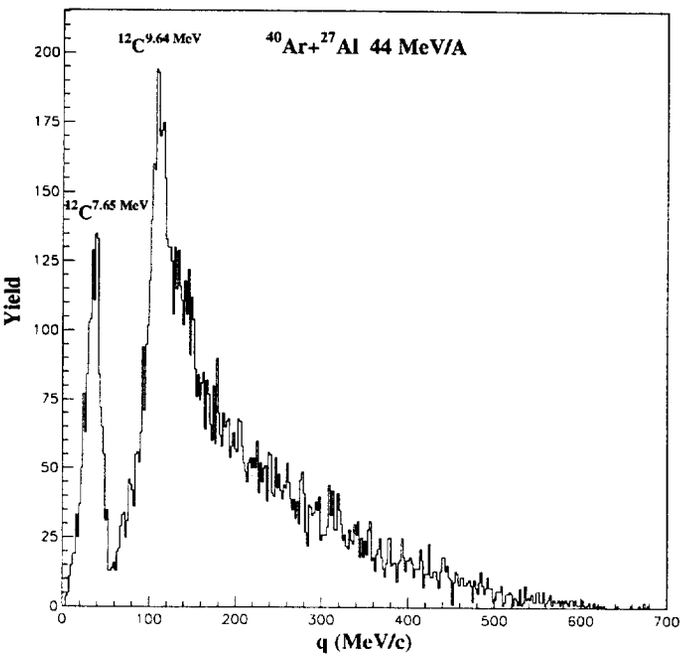

Figure 10: Relative momenta distribution for an α particle and a ^{8}Be g.s. nucleus. The two main excited levels in the primary ^{12}C nucleus are shown.

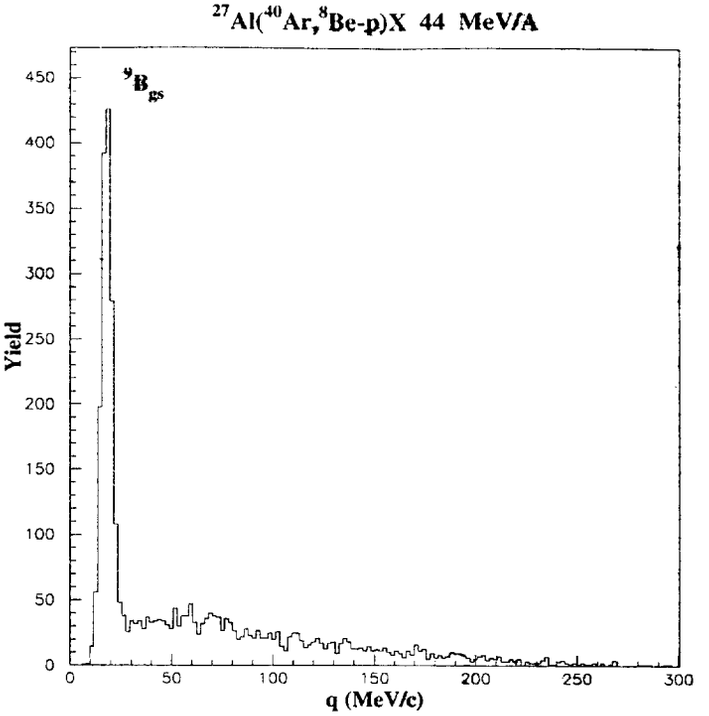

Figure 11: Relative momentum distribution for a proton and a ^{8}Be g.s. nucleus. The intense peak at low q value is due to the ^{9}B g.s. decay.

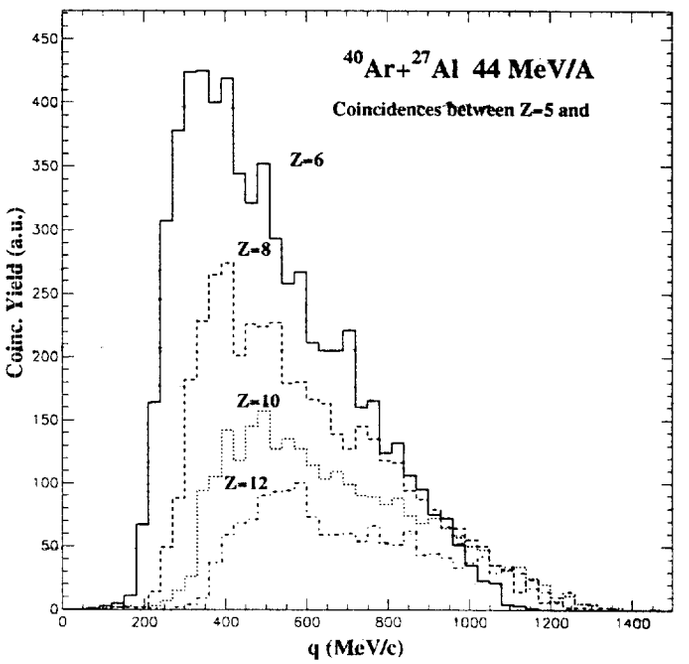

Figure 12: Relative momentum q distribution for Z=5 PLF in coincidence with Z=6,8,10,12 PLFs detected in the forward wall.

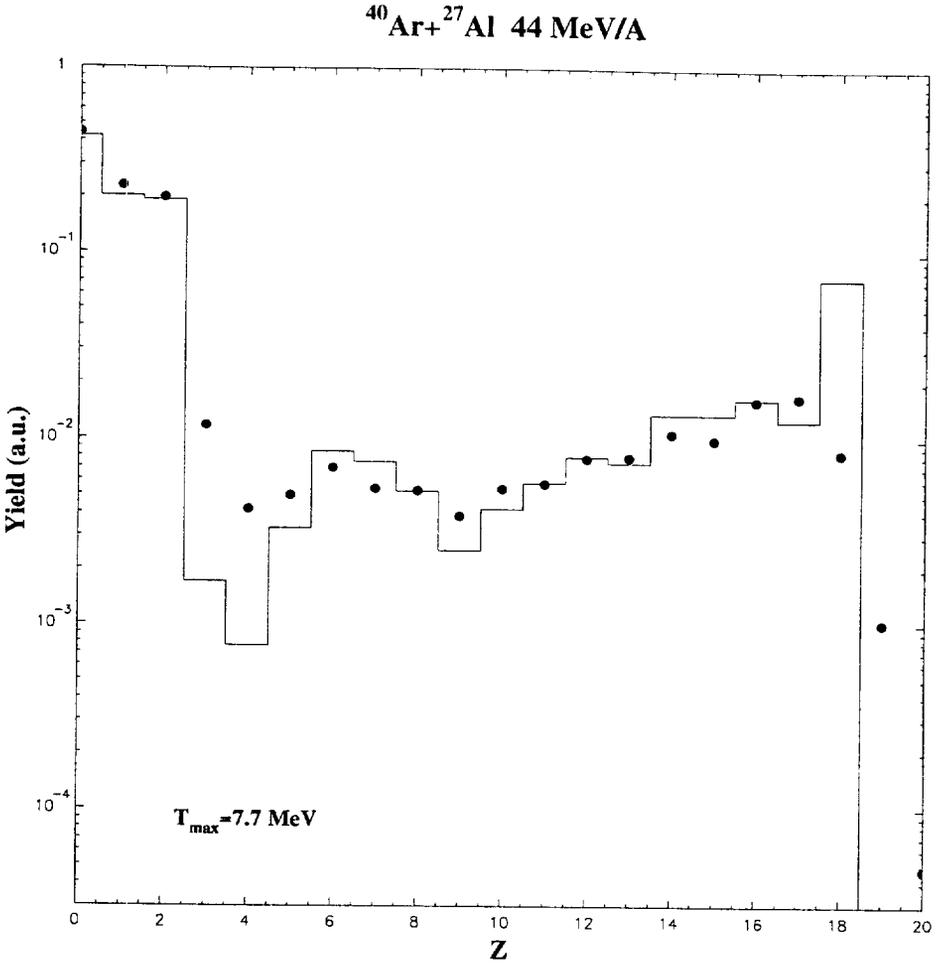

Figure 13: Experimental charge distribution for PLF-source particles (Z=0 refers to neutrons). The histogram is the result of a multisequential decay calculation with a flat temperature distribution from 0 to T_{max}= 7.7 MeV (see text).